ORIGINAL PAPER

Evaluating the application of branched tetraether proxies in surface soils along the altitudinal transect at Mount Dabie, China

Li- Huan Deng[1] · Feng-Hui Zou[2] · Huan Yang[3] · Feng Li[4]

Abstract

The branched glycerol dialkyl glycerol tetraethers (brGDGTs) are a series of bacterial membrane lipids commonly proposed as a proxy for estimating mean annual air temperature (MAAT) and pH. The biochemical response to moisture was also assumed to need to maintain the bacterial membrane integrity in arid and humid terrestrial environments. Here, we test the impact of soil chemical parameters, including pH, temperature, and moisture, on brGDGT distributions along altitudinal transect at Mount (Mt.) Dabie. The proxies (CBT, CBT′, IBT, and IR_{6ME}) are significant correlated with measured soil pH values ($R^2 = 0.62$, 0.60, 0.79, 0.64, respectively), implying the application of these proxies for pH reconstructions. Although the certain degree of scatter between brGDGT-derived temperature and altitude ($R^2 = 0.62$) may be attributed to the soil water content, the MBT'_{5ME}-derived temperature lapse rate (-6.4 °C/1000 m) resembles the measured mean annual air temperature (MAAT) lapse rate (-5.7 °C/1000 m), which suggest the MBT'_{5ME} index is mainly controlled by the MAAT values. The MBT'_{5ME} index is mainly controlled by the MAAT values in the north subtropical humid climate. The physiological alteration rather than community change may be the main mechanism underlying the variation in the MBT'_{5ME} paleothermometer along Mt. Dabie.

Keywords BrGDGTs · Attitudinal transect · Temperature · Soil pH · Soil water content

Highlights
• The CBT, CBT′, IR6ME, and IBT proxies have the large potential of paleo-pH reconstruction.
• The reconstructed MAATs from MBT′5ME are well correlated with altitude.
• The MBT′5ME proxy has a wide application of continental palaeothermometer.

✉ Feng-Hui Zou
  fhz1990@163.com

1   School of Geography and Tourism, Huanggang Normal University, Huanggang 43800, China

2   School of Geophysics and Geomatics, China University of Geosciences, No. 388 Lumo Road, Wuhan 430074, China

3   Hubei Key Laboratory of Critical Zone Evolution, School of Geography and Information Engineering, China University of Geosciences, Wuhan 430078, China

4   Huanggang Dabieshan Global Geopark Management Center, Huanggang 438000, China

Introduction

The branched glycerol dialkyl glycerol tetraethers (brG-DGTs) are a type of bacterial membrane lipids that include multiple structural molecules, distributed ubiquitously in diverse environments. The brGDGTs can vary in the number of methyl branches, the position of the outer methyl branch, namely, 5-methyl and 6-methyl brGDGTs, and the number of cyclopentane structure (0–2) (Fig. 1). The degree of methylation (MBT) responds to mean annual air temperature (MAAT) and soil pH, and the degree of cyclization (CBT) mainly correlates with pH (Weijers et al. 2007). The modified MBT′/CBT as a temperature proxy was calibrated on the global soils (Peterse et al. 2012). New advance in chromatography methodology can separate 5-methyl and 6-methyl brGDGTs (De Jonge et al. 2013). And the methylation index of 5-methyl brGDGTs (MBT'_{5ME}) and 6-methyl brGDGTs (MBT'_{6ME}) were proposed to correlate with temperature and soil pH, respectively (De Jonge et al. 2014).

After precluding 6-methyl brGDGTs, the new MBT'_{5ME} indices can resolve the "cold temperature bias" of the MBT (MBT′)/CBT proxy in arid and semi-arid soils and produce

Fig. 1 Molecular structures of brGDGTs
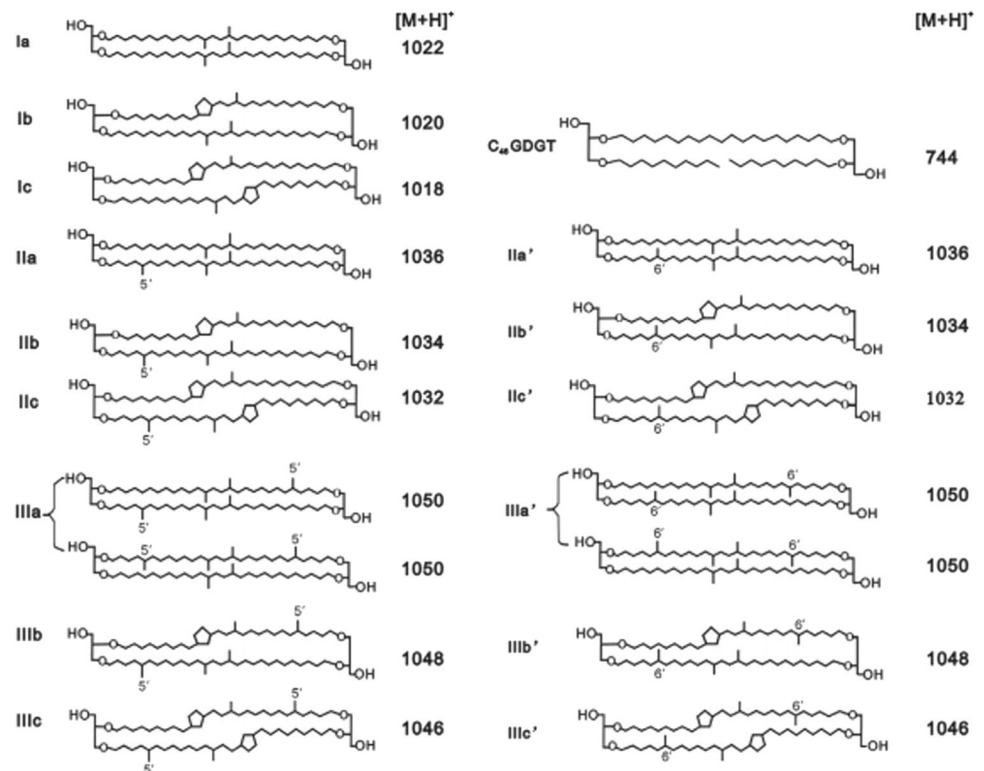
more accurate MAAT than MBT′/CBT (De Jonge et al. 2014). Recently, the pH proxies were developed including CBT′, IR_{6ME}, and IBT (De Jonge et al. 2014; Ding et al. 2015; Yang et al. 2015). Since their development, these brGDGT-based indices have been widely used to reconstruct the histories of paleotemperature and paleo-pH in varieties of terrestrial sediments (Cao et al. 2017; Deng and Jia 2018; Inglis et al. 2017; Peterse et al. 2014; Schouten et al. 2013; Wang et al. 2020a; Zhuang et al. 2019).

The $MBT′_{5ME}$ as a temperature index has been also proven with modern soils along diverse altitudinal transects (e.g., Bai et al. 2018; Feng et al. 2019; Wang et al. 2020b; Yang et al. 2015) and was promising for reconstructing paleoaltimetry due to the temperature lapse rate with height (Bai et al. 2018; Chen et al. 2019, 2020).

However, studies also speculate that non-temperature factors (e.g., soil water content, soil pH value) cause the relatively wide scatter of the $MBT′_{5ME}$ derived MAAT versus temperature (Chen et al. 2021; Dang et al. 2016; De Jonge et al. 2021). Besides, vegetation types covering on soil (Jaeschke et al. 2018; Liang et al. 2018) affect the accuracy of $MBT′_{5ME}$ temperature reconstruction. Earlier, Weijers et al. (2007) found changes in brGDGT distributions in response to environmental factors including temperature and pH, possibly reflecting homeoviscous adaptation (Chen et al. 2022; Halamka et al. 2023; Naafs et al. 2017; Weijers et al. 2007), or driven by a shift

in the bacterial community (Chen et al. 2022; De Jonge et al. 2019). Furthermore, since the bacteria producing brGDGTs has not yet been identified (Oppermann et al. 2010; Weijers et al. 2009, 2006, 2010), soil parameters may influence bacterial communities, which need more microbiological research.

The $MBT′_{5ME}$ index has been widely used for reconstruction of mean annual temperature (Wang et al. 2020a, 2018; Yang et al. 2015; Zhuang et al. 2019). However, the soil pH and moisture limit may change the response of MBT'_{5ME} to environmental factors and produce the abnormal $MBT′_{5ME}$-derived MAATs on a large spatial scale (Chen et al. 2021; De Jonge et al. 2021; Li et al. 2018; Naafs et al. 2017). Recently, the large-scale changes of soil pH were found to impact the $MBT′_{5ME}$ values (De Jonge et al. 2021). Under arid conditions, the $MBT′_{5ME}$ values respond to the non-temperature parameter, such as precipitation and soil water content as the restricted factor (Chen et al. 2021; Dang et al. 2016). In contrast, the soil water content also impacted on the methylation index of brGDGTs in cold-humid climate (Li et al. 2018). Due to the large heterogeneity of environmental variables, the $MBT′_{5ME}$ proxy showed the same respond to soil water content, but this remains to be tested in more terrestrial environments. Here, we collected soils from various heights at Mount (Mt.) Dabie (China), where temperature and precipitation conditions gradually change, to

investigate the biochemical response of brGDGTs in surface soils to the soil pH, temperature, and moisture.

Study area and method

Study area and sampling

In the main peak area of Mt. Dabie at the junction of Hubei and Anhui provinces (115°45′28.6″—115°50′57.6″E, 31°02′56″—31°14′01.7″N), a total of 12 surface soils were collected with a shovel with depth of less than 5 cm at various elevations, ranging from 338.9 to 1593.2 m (Fig. 2a–b; Table 1). They were collected after the removal of the litter layer and were combined to form a composite sample away from places with great influence of human activities. Altitude was obtained from a portable GPS (Garmin) with a precision of ± 10 m. Upon arrival at the laboratory, they were stored at -20 °C until analysis. The measured mean annual air temperatures in the study area are from climate data of the various altitude for weather stations nearby: Wujiashan monitoring site, Huanggang (114.54°, 30.26°), Huoshan (116.19°, 31.24°), Jinzhai (115.53°, 31.41°), Yingshan (115.4°, 30.44°), and Yuexi (116.22°, 30.52°). Samples were stored at -20 °C and weighted (W_o). Samples were then freeze-dried and weighted again to obtain the dry weight (W_d). Soil water content (SWC) can be calculated from the equation:
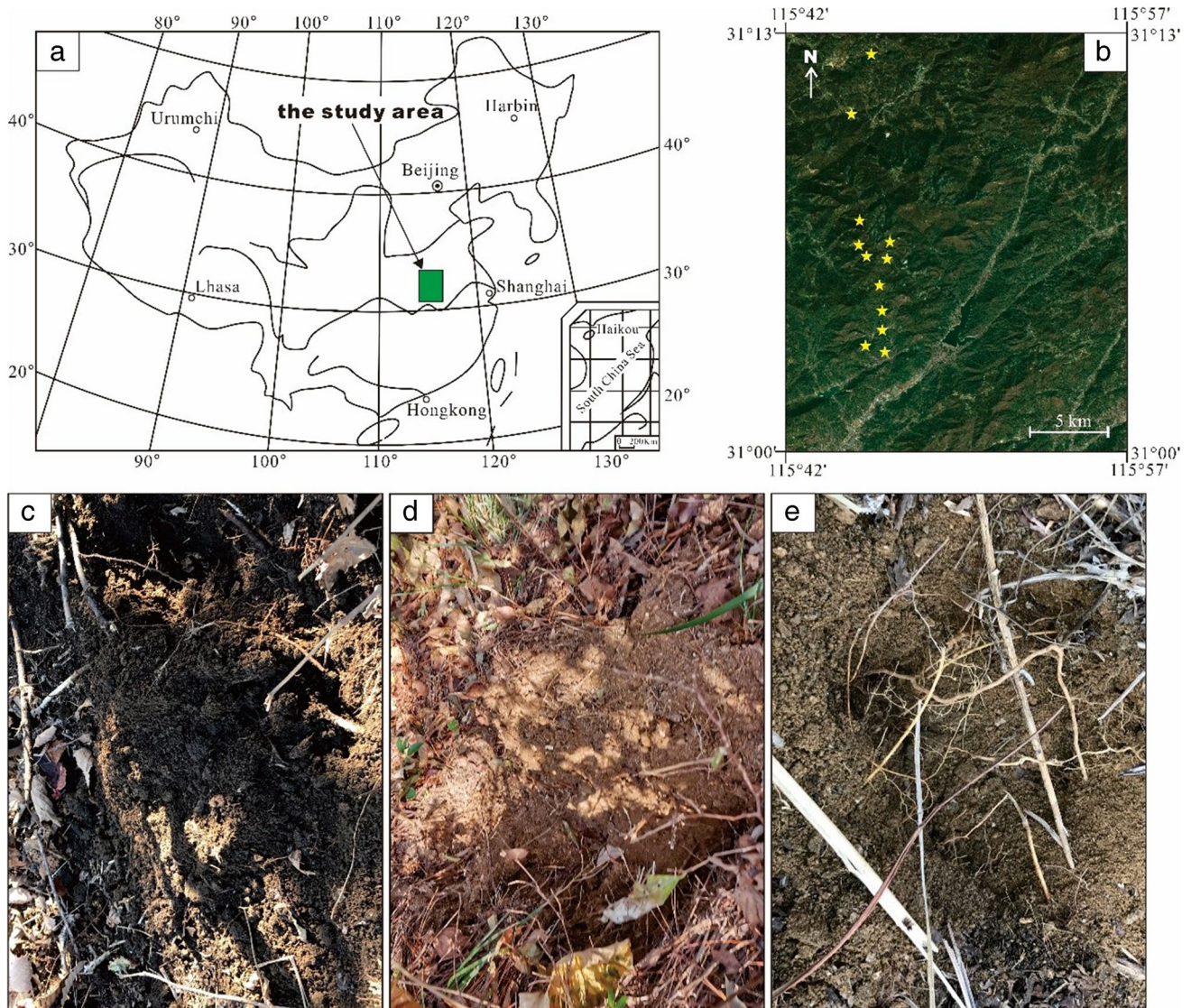
$$SWC = (W_o - W_d)/W_o \tag{1}$$

Fig. 2 **a** The location of Mt. Dabie. **b** The location of sampling sites. **c–e** Black clunamon soil at DBS45 site, sandy clunamon soil at DBS209 site, and yellow clunamon soil at DBS39 site, respectively

Table 1 Sample information of surface soils from Mt. Dabie

Number	Altitude (m)	Longitude	Latitude	Plant type	Soil type	SWC (%)	PH
DBS39	338.9	115°49′25″	31°04′24″	Mixed evergreen and deciduous broad-leaved forest	Yellow clunamon soil	5.9	6.16
DBS 37	420.7	115°49′02″	31°04′48″	Broadleaved deciduous forest	Sandy clunamon soil	5.5	6.33
DBS 75	453.0	115°49′30″	31°13′15″	Broadleaved deciduous forest	Sandy clunamon soil	14.2	5.78
DBS 213	533.7	115°48′30″	31°06′01″	Broadleaved deciduous forest	Yellow clunamon soil	20.0	5.66
DBS 209	626.1	115°48′16″	31°06′04″	Broadleaved deciduous forest	Sandy yellow clunamon soil	23.1	5.71
DBS 207	688.8	115°47′58″	31°06′06″	Broadleaved deciduous forest	Sandy yellow clunamon soil	15.1	5.97
DBS 202	828.7	115°47′27″	31°05′50″	Broadleaved deciduous forest	Sandy yellow clunamon soil	16.1	5.70
DBS 63	913.3	115°49′30″	31°08′03″	Broadleaved deciduous forest	Yellow clunamon soil	16.7	5.92
DBS 26	1068.8	115°47′05″	31°06′05″	Deciduous forest	Sandy yellow clunamon soil	13.8	4.60
DBS 18	1306.3	115°46′44″	31°06′08″	Deciduous forest	yellow clunamon soil	14.3	5.06
DBS 49	1483.9	115°46′10″	31°06′41″	Needle deciduous shrub	Brown soil	32.1	5.76
DBS 45	1593.2	115°46′02″	31°06′29″	Deciduous coniferous forest	Black clunamon soil	26.4	5.81

Experimental method

The improved experiment extraction method referred to Wang et al. (2017). Frozen soil samples were freeze-dried and homogenized, and ultrasonically extracted for lipids (4×) with a mixture of the phosphate buffer-dichloromethane (DCM) -methanol (MeOH) mixture (0.8:1:2, v/v/v; 2×) and the trichloroacetic acid buffer-DCM-MeOH mixture (0.8:1:2, v/v/v; 2×) and all extractions were combined in a 500-ml separator funnel after centrifugation. The DCM-MeOH-ultrapure water (H_2O) was adjusted to 1:1:0.9 (v/v/v) after adding ultrapure water and dichloromethane to all extractions, and the DCM part was combined by 3 times. The apolar lipid fraction containing GDGTs was separated over an active silica column with ethyl acetate (EtOA) as the eluent (Wang et al. 2017). The C_{46} GDGT standard was added to the extraction after through a 0.45-μm, 4-mm diameter PTFE filter. GDGTs were analyzed using an Agilent 1200 series high-performance liquid chromatography–atmospheric pressure chemical ionization-6460A triple quadruple mass spectrometry (HPLC–APCI-MS^2). GDGT separation was achieved using two BEH HILIC silica columns in tandem (150 mm×2.1 mm, 1.7 μm, Waters) maintained at 40 °C (Hopmans et al. 2016). Samples were dissolved by a mixture of n-hexane: isopropanol (v/v,99:1). Flow rate was

0.3 ml/min, and the injection volume was 10 μl. Samples were eluted with n-hexane(A) and n-hexane: isopropanol (v/v, 9:1; B). The elution gradient was used: 82% A and 18% B for 25 min, %B increased to 35% among 25–50 min, 100% among 50–80 min, and decreased back to 18% among 80–90 min, kept 18%B for the last 20 min.

Calculation of brGDGT-based proxies

CBT, MBT′$_{5ME}$ and CBT′ (newly defined CBT) indices were calculated according to Weijers et al. (2007) and De Jonge et al. (2014).

$$CBT = log[(Ib + IIb + IIb') / (Ia + IIa + IIa')] \quad (2)$$

$$MBT' = (Ia + Ib + Ic)$$
$$/(Ia + Ib + Ic + IIa + IIb + IIc + IIa' + IIb' + IIc' + IIIa + IIIa') \quad (3)$$

$$MBT'_{5ME} = (Ia + Ib + Ic)/(Ia + Ib + Ic + IIa + IIb + IIc + IIIa) \quad (4)$$

$$CBT' = log[(Ic + IIa' + IIb' + IIc' + IIIa' + IIIb' + IIIc')$$
$$/(Ia + IIa + IIIa)] \quad (5)$$

The relative amount of C6- versus C5-methylated brGDGTs (i.e., IR_{6ME} index) was calculated according to De Jonge et al. (2014):

$$IR6ME = (IIa' + IIb' + IIc' + IIIa' + IIIb' + IIIc')$$
$$/(Ia + Ib + Ic + IIa + IIb + IIc + IIIa + IIIb + IIIc + IIa' + IIb' + IIc' + IIIa' + IIIb' + IIIc') \quad (6)$$

The IBT index (isomerization of branched tetraethers) was defined as the abundant ratio of noncyclopentyl 6-methyl to 5-methyl brGDGTs and was calculated according to Ding et al. (2015).

$$IBT = -log[(IIa' + IIIa')/(IIa + IIIa)] \quad (7)$$

The community index (CI) was used to evaluate the impact of bacterial community shift on the brGDGT

signature and was calculated according to De Jonge et al. (2019).

$$CI = Ia/(Ia + IIa + IIIa) \tag{8}$$

Statistical analysis

The squared Pearson correlation coefficient (R^2) and p-value of correlation test between paired samples are reported when performing linear regressions. The linear regressions between environmental variables and brGDGT-derived indices were performed using the Microsoft 365 excel software. A Pearson's coefficient (p-value) < 0.05 means the correlation is significant. Boxplot of the community index was performed using the Origin software.

Results and discussion

The distribution of brGDGTs

All 5- and 6-methyl brGDGTs were separated in all samples. At low altitude, brGDGT-I series is generally the most abundant (Fig. 3a), and the proportion of brGDGT-II series obviously increases at high altitude (Fig. 3b). Among the fifteen brGDGTs, their relative abundances in average in Mt. Dabie
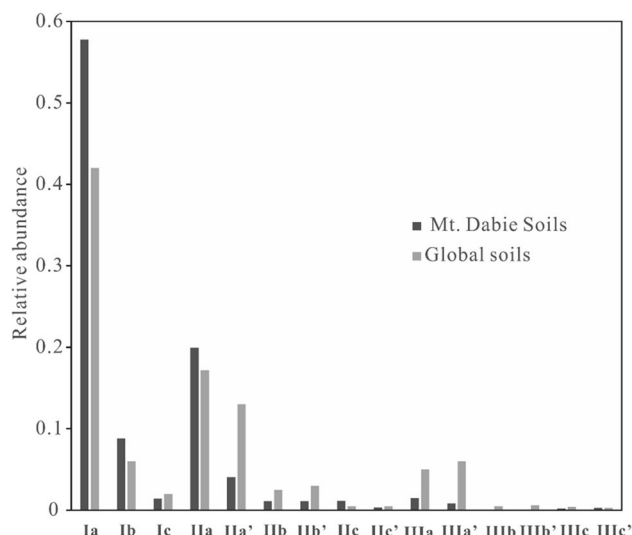

Fig. 4 The abundances of 15 brGDGTs in Mt. Dabie and global soils (De Jonge et al. 2014)

are shown in Fig. 4. The abundances of 5-methyl brGDGTs (avg. 25.7%) were higher than that of 6-methyl brGDGTs (avg. 7.0%). The most dominant brGDGTs were Ia, Ib, and IIa compounds, with the total abundances of 80% in average, and the abundances of tetramethyl brGDGTs (Ia, Ib and Ic) were notably high compared to pentamethyl and hexamethyl

Fig. 3 HPLC-APCI/MS base peak chromatograms showing the distribution of brGDGTs at (**a**) low and (**b**) high latitudes of Mt. Dabie
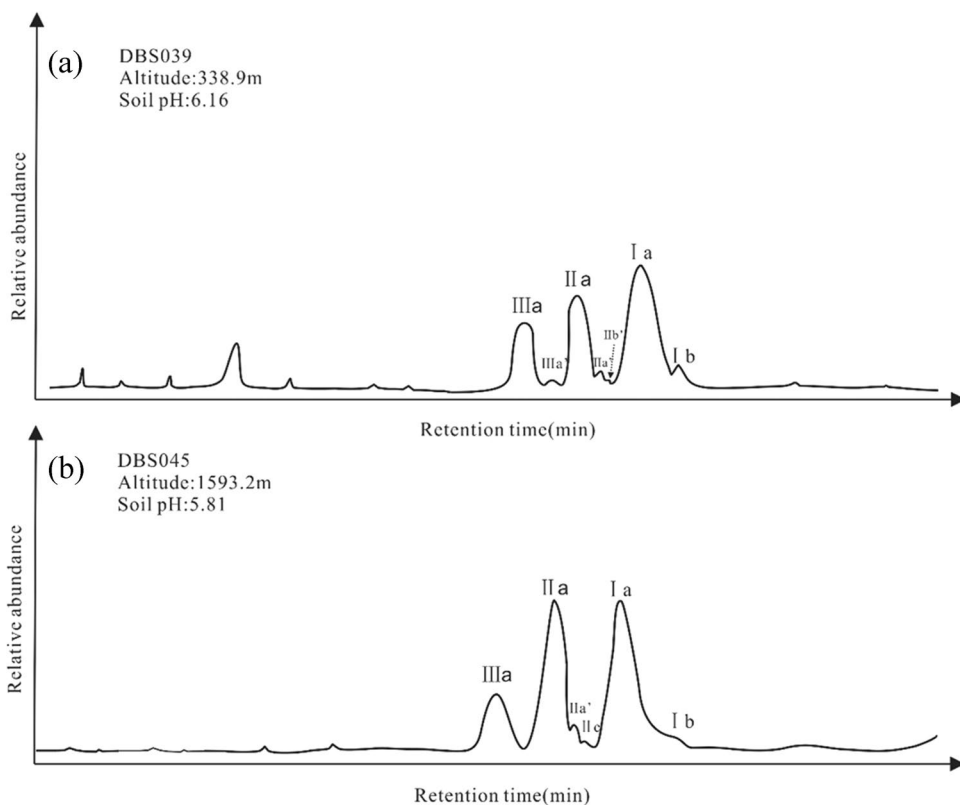
brGDGTs. Meanwhile, acyclic brGDGT-I, II, and III (Ia, IIa, IIa′, IIIa, IIIa′) were most abundant, followed by cyclic brGDGTs and brGDGTs with two cyclopentyl rings successively. They are similar to the global soil brGDGT distribution (Fig. 4, De Jonge et al. 2014). According to the global soil dataset (De Jonge et al. 2014), the majority of global soil pH focused on the range of 4~7, and a large of MAP are above 500 mm. In the study, the scope of soil moisture and soil pH from Mt. Dabie correspond to that of global soils. So, the global temperature calibration may be valid to estimate temperature. In addition, there are also some differences between the distribution of soil brGDGT abundance at Mt. Dabie and the average abundance of brGDGTs in the global soil, which is due to the differences between the average levels of temperature and pH of the global and that of the regional.

BrGDGT-based proxies

The CBT index ranged from 0.41 to 1.61, with an average of 1.01, and the newly CBT′ index varied from -1.64 to -0.63, with an average of -1.06. The CBT′-derived pH values ranged from 4.55 to 6.15, with an average of 5.46. The MBT′$_{5ME}$ indices varied from 0.47 to 0.85, with an average of 0.73 (Table 2).

The unidentified bacterial producing brGDGTs can respond to several environmental factors simultaneously, such as soil temperature, soil water content, and soil pH value. After precluding 6-methyl brGDGTs, the newly MBT′$_{5ME}$ index is only correlated with MAAT, no longer related to soil pH (De Jonge et al. 2014). Here, the CBT′ index and the measured pH showed no variation trend (Fig. 5a, c). With the increase of altitude, the rate of the measured annual mean temperature decrease at nearby weather station was 5.7 °C/ km and the soil water content exhibited a moderate increasing trend. The CBT, CBT′, IBT, and IR$_{6ME}$ proxies were well

correlated with pH, with their high coefficients ($R^2 = 0.62$, 0.60, 0.79, 0.64, respectively; Fig. 6a). The decrease of MBT′$_{5ME}$ with increasing elevation (Fig. 5a) is therefore very likely associated with the decrease of temperature and not affected by soil pH, which suggests that the MBT′$_{5ME}$ index may be valid for temperature estimation.

The relatively low soil water content in areas with the mean annual precipitation (MAP) > 1000 mm may be related to the soil containing sand from granite weathering. The physiological response of brGDGT-producing microorganisms was not affected by limiting environmental factors in warm and humid climate regimes, and the MBT′$_{5ME}$ index was primarily controlled by temperature. Nevertheless, the MBT′$_{5ME}$ has a rather weakly linear correlation with SWC ($R^2 = 0.34$; $p < 0.001$; Fig. 6b), for one reason of causing the wide scatter between the MBT′$_{5ME}$-temperature and elevation. And it apparently is different the previous finding that the MBT′$_{5ME}$ showed correlation with soil water content but no relationship with MAAT in cold and humid Mt. Changbai, where the freezing condition by the soil moisture content may restrict the growth of microorganisms (Li et al. 2018). Besides, the discrepancy between soil mean annual temperature and MAAT has been suggested to be one possible reason for the scatter in the calibrations of new brGDGT temperature proxies (De Jonge et al. 2014; Ding et al. 2015; Yang et al. 2015), but no soil temperature data at Mount Dabie hampers a discussion of the relationship between the MBT′$_{5ME}$ and soil.

Based on the global calibration by De Jonge et al. (2014), the MBT′$_{5ME}$-derived temperature ranged from 6.1 to 18.3 °C with increasing elevation, showing a lapse rate of -6.4 °C/km ($R^2 = 0.62$). Both the MBT′$_{5ME}$ temperature and its lapse rate were consistent with the measured temperature and lapse rate (-5.7 °C/1000 m, $R^2 = 0.95$; Fig. 6c). Moreover, compared to the classic MBT′ index, MBT′$_{5ME}$ indices appear well-correlated with MAAT/altitude, and their temperature lapse rates are closer to the

Table 2 The brGDGT climate ratios and reconstructions for soils along an altitudinal transect of Mt. Dabie

| Sample no	CBT	CBT′	MBT′	MBT′$_{5ME}$	MBT′$_{5ME}$-MAAT	CBT′-pH
DBS39	0.42	-0.64	0.68	0.76	15.3	6.13
DBS37	0.67	-0.63	0.67	0.78	16.2	6.15
DBS75	1.21	-1.18	0.79	0.84	17.8	5.28
DBS213	1.60	-1.42	0.79	0.80	16.8	4.89
DBS209	1.53	-1.25	0.82	0.85	18.3	5.16
DBS207	0.81	-0.95	0.69	0.73	14.5	5.63
DBS202	1.10	-1.38	0.78	0.80	16.8	4.95
DBS63	0.76	-0.81	0.68	0.75	14.9	5.86
DBS26	1.61	-1.38	0.65	0.67	12.5	4.96
DBS18	1.32	-1.64	0.73	0.74	14.7	4.55
DBS49	0.65	-0.78	0.43	0.47	6.1	5.91
DBS45	0.41	-0.66	0.53	0.60	10.4	6.10
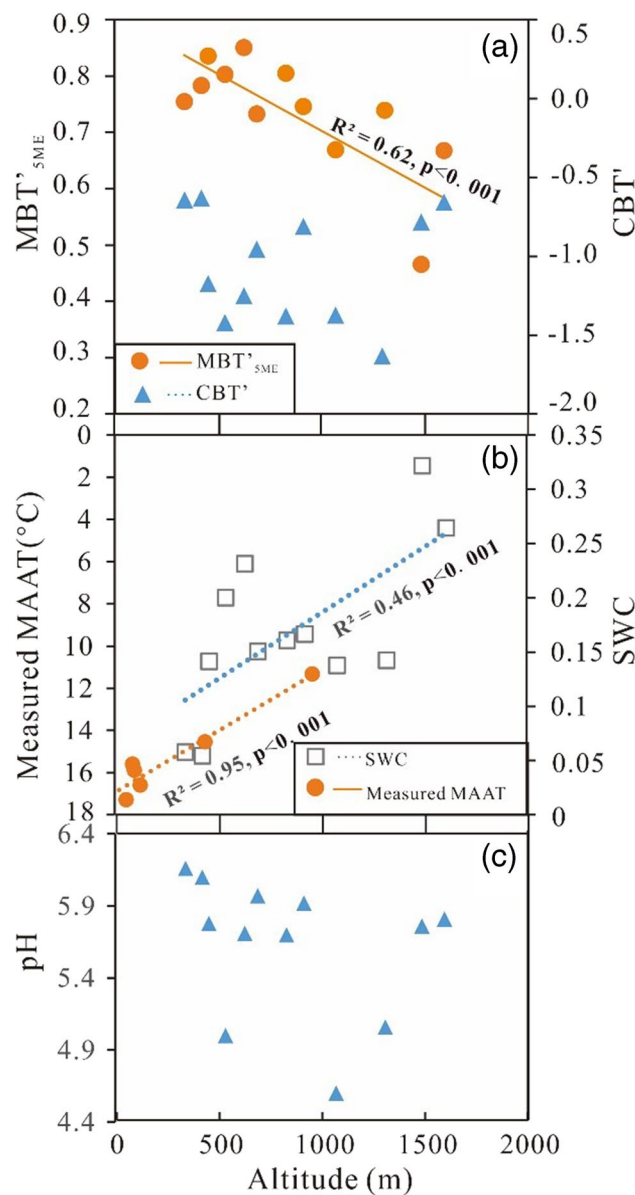
Fig. 5 **a** Linear correlations between MBT'_{5ME}, CBT' for soils from Mt. Dabie, and altitude. **b** Linear correlations between the measured MAAT, SWC, and altitude. **c** Soil pH vs. altitude

Fig. 6 **a** Linear correlations between CBT, CBT, IBT, and IR_{6ME} for soils from Mt. Dabie and altitude. **b** The linear relationship of MBT'_{5ME} and SWC. **c** Comparison between the estimated MAAT using the MBT'_{5ME} proxy and the measured MAAT at nearby weather stations

measured (Fig. 6c). Similarly, the utility of the MBT'_{5ME} paleothermometer in diverse altitudinal slope environments has been previously reported (Bai et al. 2018; Feng et al. 2019; Yang et al. 2015). In addition, the variation of vertical of plant type is evergreen-deciduous broadleaved mixed forest and deciduous broadleaved forest in Mt. Dabie. The different soil types and vegetation types along mountainous slope may lead to the different composition of bacterial membrane lipids synthesized by microorganisms adapting to the growth environment (Fig. 2c–e). In humid subtropical climate, although different vegetation and soil type composition and vertical zone changes along altitudinal slopes,
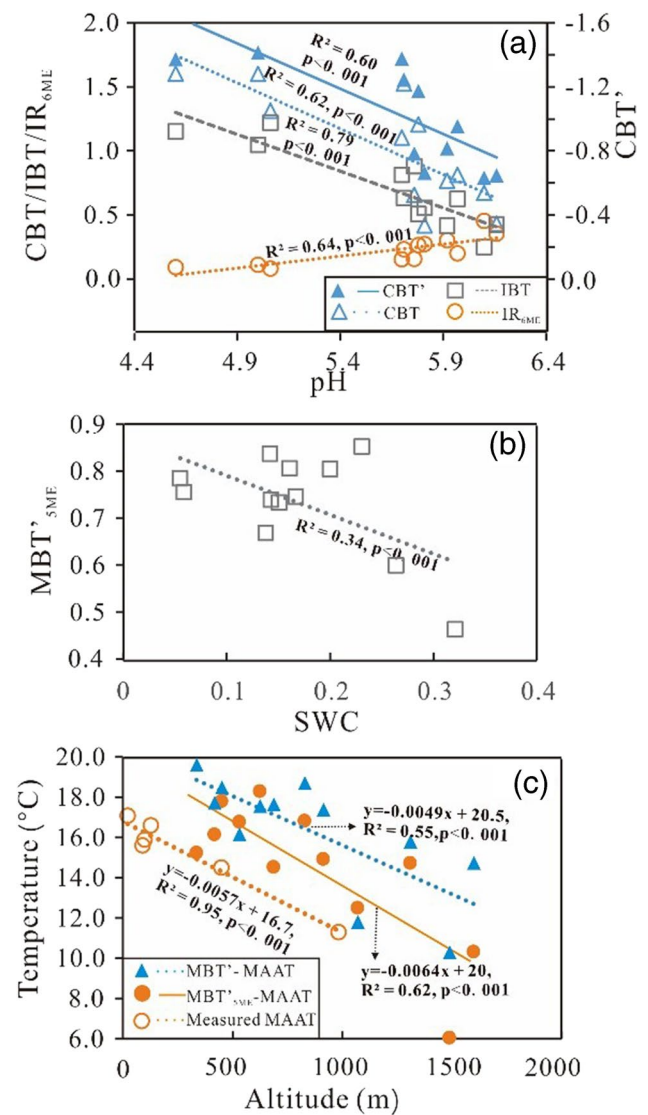
brGDGT-based temperature lapse rate is stable, indicating that vertical vegetation and soil type have little influence on brGDGT temperature proxy (Anderson et al. 2014; Coffinet et al. 2014; Damste et al. 2008; Ernst et al. 2013; Liu et al. 2013; Peterse et al. 2009). Recently, the obviously different MAAT lapse rates in subtropical China were observed, which be primarily caused by differences in latitudinal temperature and/or moisture conditions (Wang et al. 2020b).

The scatter in the MBT'_{5ME} value-altitude relationship here ($R^2 = 0.62$, $p < 0.01$; Fig. 6a) accords with the previous reports showing R^2 values varying from 0.55 to 0.9 (Wang et al. 2018; Yang et al. 2015). Several other factors, such as seasonality, oxygen content, and slope surface, have been
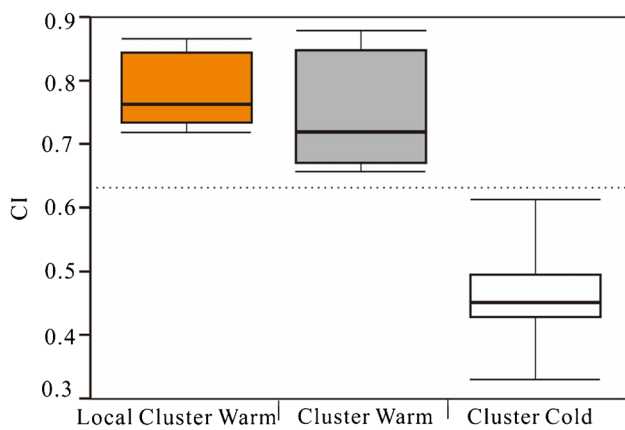
Fig. 7 Boxplot of the community index (CI [Eq. (6)]) values of the Mt. Dabie soils, for local cluster warm (yellow); CI values of ForHot soils (De Jonge et al. 2019) for local cluster warm (grey), and local cluster cold (white). The cut-off value of 0.64 is indicated

suggested to contribute to the wide scatter (Chen et al. 2021; Crampton-Flood et al. 2020; Deng et al. 2016; Jaeschke et al. 2018; Wang et al. 2018; Yang et al. 2015).

In a set of globally distributed soils, the MBT'_{5ME} ratio reveals a strong temperature dependency, which is the basis of the temperature calibration developed by Naafs et al. (2017). However, at local scales, the bacterial community effect rather than physiological plasticity can dominate the distribution of brGDGTs (De Jonge et al. 2019). Moreover, it is noteworthy that the community index (CI) with a threshold of 0.64 was recently used to divide soils into cluster warm and cluster cold based on their lipid distribution, with greater CI values corresponding to warmer environments (De Jonge et al. 2019). Therefore, we evaluate the impact of microbial community on the variation in the MBT'_{5ME} paleothermometer. Firstly, our CI values from Mt. Dabie surface soils are between 0.34 and 0.86 (Fig. 7). Among them, only two CI values of the DBS49 and DBS45 samples are under 0.64, corresponding to colder environments at the highest altitude of 1483.9 m and 1593.2 m. However, a more detailed discussion on soil bacterial communities is hampered due to lack of the genetic data for soils from Mt. Dabie. Secondly, in altitudinal or latitudinal transects with a large temperature or pH gradient, the effect of these environmental factors on brGDGT distribution overwhelmingly exceeds the community effect, resulting in significant correlations between brGDGT distribution and temperature or pH (Anderson et al. 2014; Bai et al. 2018; Feng et al. 2019; Yang et al. 2015). The MBT'_{5ME} temperature lapse rate approximate to the measured temperature lapse rate suggests that the MBT'_{5ME} index–derived MAAT, and its temperature lapse rates can be valid along the altitudinal slope (Fig. 6c). Finally, The MBT'_{5ME} index in cultured strain Candidatus Solibacter usitatus Ellin6076 is primarily determined by temperature from a physiological perspective, in agreement with the global soil-derived

MBT'_{5ME} proxy for temperature (Chen et al. 2022). Therefore, this implies that physiological alteration rather than community change can be the main mechanism underlying the variation in the MBT'_{5ME} paleothermometer along Mt. Dabie.

Conclusion

1. The CBT, CBT′, IR_{6ME}, and IBT proxies all showed the correlation with soil pH.
2. The MBT'_{5ME}-derived temperatures are slightly higher than the measured values.
3. The MBT'_{5ME} values were primarily dependent on the temperature in the warm and humid climate. Although there is a wide scatter in the correlation between MBT'_{5ME}-derived temperature and altitude, which may be caused by the soil water content, the MBT'_{5ME} derived a temperature lapse rate resembles the measured lapse rate (-6.4 °C/1000 m and -5.7 °C/1000 m, respectively).

Author contribution All authors contributed to the field sample collecting. Li-Huan Deng and Feng-Hui Zou completed the study design. Material preparation, data collection, and analysis were performed by Li-Huan Deng, Feng-Hui Zou, and Huan Yang. The first draft of the manuscript was written by Li-Huan Deng. Li-Huan Deng and Feng-Hui Zou completed the revision work. All authors read and approved the final manuscript.

Data Availability The authors confirm that the data supporting the finding of this study are available within the article. Raw data that support the findings of this study are available from the corresponding author, upon reasonable request.

Declarations

Competing interests The authors declare no competing interests.

References

Anderson VJ, Shanahan TM, Saylor JE, Horton BK, Mora AR (2014) Sources of local and regional variability in the MBT′/CBT

paleotemperature proxy: Insights from a modern elevation transect across the Eastern Cordillera of Colombia. Org Geochem 69:42–51. https://doi.org/10.1016/j.orggeochem.2014.01.022

Bai Y, Chen CH, Xu Q, Fang XM (2018) Paleoaltimetry potentiality of branched GDGTs from Southern Tibet. Geochem Geophys Geosyst 19:551–564. https://doi.org/10.1002/2017gc007122

Cao JT, Rao ZG, Jia GD, Xu QH, Chen FH (2017) A 15 ka pH record from an alpine lake in north China derived from the cyclization ratio index of aquatic brGDGTs and its paleoclimatic significance. Org Geochem 109:31–46. https://doi.org/10.1016/j.orggeochem.2017.02.005

Chen CH, Bai Y, Fang XM, Guo HC, Meng QQ, Zhang WL, Zhou PC, Murodov A (2019) A Late Miocene terrestrial temperature history for the Northeastern Tibetan Plateau's period of tectonic expansion. Geophys Res Lett 46:8375–8386. https://doi.org/10.1029/2019gl082805

Chen CH, Bai Y, Fang XM, Xu Q, Zhang T, Deng T, He JK, Chen QH (2020) Lower-altitude of the Himalayas before the mid-Pliocene as constrained by hydrological and thermal conditions. Earth Planet Sc Lett 545:11. https://doi.org/10.1016/j.epsl.2020.116422

Chen CH, Bai Y, Fang XM, Zhuang GS, Khodzhiev A, Bai XJ, Murodov A (2021) Evaluating the potential of soil bacterial tetraether proxies in westerlies dominating western Pamirs, Tajikistan and implications for paleoenvironmental reconstructions. Chem Geol 559:119908. https://doi.org/10.1016/j.chemgeo.2020.119908

Chen YF, Zheng FF, Yang H, Yang W, Wu RJ, Liu XY, Liang HY, Chen HH, Pei HY, Zhang CL, Pancost RD, Zeng ZR (2022) The production of diverse brGDGTs by an Acidobacterium providing a physiological basis for paleoclimate proxies. Geochim Cosmochim Ac 337:155–165. https://doi.org/10.1016/j.gca.2022.08.033

Coffinet S, Huguet A, Williamson D, Fosse C, Derenne S (2014) Potential of GDGTs as a temperature proxy along an altitudinal transect at Mount Rungwe (Tanzania). Org Geochem 68:82–89. https://doi.org/10.1016/j.orggeochem.2014.01.004

Crampton-Flood ED, Tierney JE, Peterse F, Kirkels FMSA, Damste JSS (2020) BayMBT: A Bayesian calibration model for branched glycerol dialkyl glycerol tetraethers in soils and peats. Geochim Cosmochim Ac 268:142–159. https://doi.org/10.1016/j.gca.2019.09.043

Damste JSS, Ossebaar J, Schouten S, Verschuren D (2008) Altitudinal shifts in the branched tetraether lipid distribution in soil from Mt. Kilimanjaro (Tanzania): Implications for the MBT/CBT continental palaeothermometer. Org Geochem 39:1072–1076. https://doi.org/10.1016/j.orggeochem.2007.11.011

Dang XY, Yang H, Naafs BDA, Pancost RD, Xie SC (2016) Evidence of moisture control on the methylation of branched glycerol dialkyl glycerol tetraethers in semi-arid and arid soils. Geochim Cosmochim Ac 189:24–36

De Jonge C, Hopmans EC, Stadnitskaia A, Rijpstra WIC, Hofland R, Tegelaar E, Sinninghe Damsté JS (2013) Identification of novel penta- and hexamethylated branched glycerol dialkyl glycerol tetraethers in peat using HPLC–MS2, GC–MS and GC–SMB-MS. Org Geochem 54:78–82. https://doi.org/10.1016/j.orggeochem.2012.10.004

De Jonge C, Hopmans EC, Zell CI, Kim JH, Schouten S, Sinninghe Damsté JS (2014) Occurrence and abundance of 6-methyl branched glycerol dialkyl glycerol tetraethers in soils: Implications for palaeoclimate reconstruction. Geochim Cosmochim Ac 141:97–112. https://doi.org/10.1016/j.gca.2014.06.013

De Jonge C, Kuramae EE, Radujkovic D, Weedon JT, Janssens IA, Peterse F (2021) The influence of soil chemistry on branched tetraether lipids in mid- and high latitude soils: implications for brGDGT- based paleothermometry. Geochim Cosmochim Ac 310:95–112. https://doi.org/10.1016/j.gca.2021.06.037

Deng LH, Jia GD (2018) High-relief topography of the Nima basin in central Tibetan Plateau during the mid-Cenozoic time. Chem Geol 493:199–209. https://doi.org/10.1016/j.chemgeo.2018.05.041

Deng L, Jia G, Jin C, Li S (2016) Warm season bias of branched GDGT temperature estimates causes underestimation of altitudinal lapse rate. Org Geochem 96:11–17. https://doi.org/10.1016/j.orggeochem.2016.03.004

Ding S, Xu Y, Wang Y, He Y, Hou J, Chen L, He J-S (2015) Distribution of branched glycerol dialkyl glycerol tetraethers in surface soils of the Qinghai-Tibetan Plateau: implications of brGDGTs-based proxies in cold and dry regions. Biogeosciences 12:3141–3151. https://doi.org/10.5194/bg-12-3141-2015

Ernst N, Peterse F, Breitenbach SFM, Syiemlieh HJ, Eglinton TI (2013) Biomarkers record environmental changes along an altitudinal transect in the wettest place on Earth. Org Geochem 60:93–99. https://doi.org/10.1016/j.orggeochem.2013.05.004

Feng XP, D'Andrea WJ, Zhao C, Xin SZ, Zhang C, Liu WG (2019) Evaluation of leaf wax delta D and soil brGDGTs as tools for paleoaltimetry on the southeastern Tibetan Plateau. Chem Geol 523:95–106. https://doi.org/10.1016/j.chemgeo.2019.05.005

Halamka TA, Raberg JH, McFarlin JM, Younkin AD, Mulligan C, Liu XL, Kopf SH (2023) Production of diverse brGDGTs by Acidobacterium Solibacter usitatus in response to temperature, pH, and O(2) provides a culturing perspective on brGDGT proxies and biosynthesis. Geobiology 21:102–118. https://doi.org/10.1111/gbi.12525

Hopmans EC, Schouten S, Sinninghe Damsté JS (2016) The effect of improved chromatography on GDGT-based palaeoproxies. Org Geochem 93:1–6. https://doi.org/10.1016/j.orggeochem.2015.12.006

Inglis GN, Collinson ME, Riegel W, Wilde V, Farnsworth A, Lunt DJ, Valdes P, Robson BE, Scott AC, Lenz OK, Naafs BDA, Pancost RD (2017) Mid-latitude continental temperatures through the early Eocene in western Europe. Earth Planet Sc Lett 460:86–96. https://doi.org/10.1016/j.epsl.2016.12.009

Jaeschke A, Rethemeyer J, Lappé M, Schouten S, Boeckx P, Schefuß E (2018) Influence of land use on distribution of soil n-alkane δD and brGDGTs along an altitudinal transect in Ethiopia: Implications for (paleo)environmental studies. Org Geochem 124:77–87. https://doi.org/10.1016/j.orggeochem.2018.06.006

De Jonge C, Radujković D, Sigurdsson BD, Weedon JT, Janssens I, Peterse F (2019) Lipid biomarker temperature proxy responds to abrupt shift in the bacterial community composition in geothermally heated soils. Org Geochem 137 https://doi.org/10.1016/j.orggeochem.2019.07.006

Li Y, Zhao S, Pei H, Qian S, Zang J, Dang XY, Yang H (2018) Distribution of glycerol dialkyl glycerol tetraethers in surface soils along an altitudinal transect at cold and humid Mountain Changbai: Implications for the reconstruction of paleoaltimetry and paleoclimate. Sci China Earth Sci 61:925–939. https://doi.org/10.1007/s11430-017-9168-9

Liang J, Russell JM, Xie HC, Lupien RL, Si GC, Wang J, Hou JZ, Zhang GG (2018) Vegetation effects on temperature calibrations of branched glycerol dialkyl glycerol tetraether (brGDGTs) in soils. Org Geochem 127:1–11. https://doi.org/10.1016/j.orggeochem.2018.10.010

Liu WG, Wang HY, Zhang CL, Liu ZH, He YX (2013) Distribution of glycerol dialkyl glycerol tetraether lipids along an altitudinal transect on Mt. Xiangpi, NE Qinghai-Tibetan Plateau. China Org Geochem 57:76–83. https://doi.org/10.1016/j.orggeochem.2013.01.011

Naafs BDA, Gallego-Sala AV, Inglis GN, Pancost RD (2017) Refining the global branched glycerol dialkyl glycerol tetraether (brGDGT) soil temperature calibration. 106. Org Geochem 106:48–56. https://doi.org/10.1016/j.orggeochem.2017.01.009

Oppermann BI, Michaelis W, Blumenberg M, Frerichs J, Schulz HM, Schippers A, Beaubien SE, Kruger M (2010) Soil microbial community changes as a result of long-term exposure to a natural CO2 vent. Geochim Cosmochim Ac 74:2697–2716. https://doi.org/10.1016/j.gca.2010.02.006

Peterse F, van der Meer MTJ, Schouten S, Jia GD, Ossebaar J, Blokker J, Sinninghe Damsté JS (2009) Assessment of soil n-alkane dD and branched tetraether membrane lipid distributions as tools for paleoelevation reconstruction. Biogeosciences 6:2799–2807

Peterse F, van der Meer J, Schouten S, Weijers JWH, Fierer N, Jackson RB, Kim J-H, Sinninghe Damsté JS (2012) Revised calibration of the MBT–CBT paleotemperature proxy based on branched tetraether membrane lipids in surface soils. Geochim Cosmochim Ac 96:215–229. https://doi.org/10.1016/j.gca.2012.08.011

Peterse F, Vonk JE, Holmes RM, Giosan L, Zimov N, Eglinton TI (2014) Branched glycerol dialkyl glycerol tetraethers in Arctic lake sediments: Sources and implications for paleothermometry at high latitudes. J Geophys Res Biogeosci 119:1738–1754. https://doi.org/10.1002/2014jg002639

Schouten S, Hopmans EC, Damste JSS (2013) The organic geochemistry of glycerol dialkyl glycerol tetraether lipids: A review. Org Geochem 54:19–61. https://doi.org/10.1016/j.orggeochem.2012.09.006

Wang HY, Liu WG, Zhang CL (2017) Comparison of the ultrasound-assisted organic solvent extraction and modified Bligh-Dyer extraction for the analysis of glycerol dialkyl glycerol tetraethers from environmental samples Journal of Earth. Environment 8:176–184. https://doi.org/10.7515/jee201702010

Wang MY, Zong YQ, Zheng Z, Man ML, Hu JF, Tian LP (2018) Utility of brGDGTs as temperature and precipitation proxies in subtropical China. Sci Rep 8:194. https://doi.org/10.1038/s41598-017-17964-0

Wang HY, An ZS, Lu HX, Zhao ZH, Liu WG (2020a) Calibrating bacterial tetraether distributions towards in situ soil temperature and application to a loess-paleosol sequence. Quaternary Sci Rev 231:106172. https://doi.org/10.1016/j.quascirev.2020.106172

Wang MY, Yang H, Zheng Z, Tian LP (2020b) Altitudinal climatic index changes in subtropical China indicated from branched glycerol dialkyl glycerol tetraethers proxies. Chem Geol 541:119579. https://doi.org/10.1016/j.chemgeo.2020.119579

Weijers JWH, Schouten S, Hopmans EC, Geenevasen JAJ, David ORP, Coleman JM, Pancost RD, Damste JSS (2006) Membrane lipids of mesophilic anaerobic bacteria thriving in peats have typical archaeal traits. Environ Microbiol 8:648–657. https://doi.org/10.1111/j.1462-2920.2005.00941.x

Weijers JWH, Schouten S, van den Donker JC, Hopmans EC, Damste JSS (2007) Environmental controls on bacterial tetraether membrane lipid distribution in soils. Geochim Cosmochim Ac 71:703–713. https://doi.org/10.1016/j.gca.2006.10.003

Weijers JWH, Panoto E, van Bleijswijk J, Schouten S, Rijpstra WIC, Balk M, Stams AJM, Damste JSS (2009) Constraints on the biological source(s) of the orphan branched tetraether membrane lipids. Geomicrobiol J 26:402-414 Pii 913953712. https://doi.org/10.1080/01490450902937293

Weijers JWH, Wiesenberg GLB, Bol R, Hopmans EC, Pancost RD (2010) Carbon isotopic composition of branched tetraether membrane lipids in soils suggest a rapid turnover and a heterotrophic life style of their source organism(s). Biogeosciences 7:2959–2973. https://doi.org/10.5194/bg-7-2959-2010

Yang H, Lü XX, Ding WH, Lei YY, Dang XY, Xie SC (2015) The 6-methyl branched tetraethers significantly affect the performance of the methylation index (MBT′) in soils from an altitudinal transect at Mount Shennongjia. Org Geochem 82:42–53. https://doi.org/10.1016/j.orggeochem.2015.02.003

Zhuang GS, Zhang YG, Hourigan J, Ritts B, Hren M, Hou MQ, Wu MH, Kim B (2019) Microbial and geochronologic constraints on the Neogene Paleotopography of Northern Tibetan Plateau. Geophys Res Lett 46:1312–1319. https://doi.org/10.1029/2018gl081505